Electronic Supplementary Material (ESI) for Lab on a Chip.

Supplementary Information

Title: dMSCC: A microfluidic platform for microbial single-cell cultivation of *Corynebacterium glutamicum* under dynamic environmental medium conditions

Authors: Sarah Täuber[1], Corinna Golze[1], Phuong Ho[2], Eric von Lieres[2] and Alexander Grünberger[1*]

[1] *Multiscale Bioengineering, Technical Faculty, Bielefeld University, Universitätsstraße 25, 33615 Bielefeld, Germany*

[2] *Institute of Bio- and Geosciences, IBG-1: Biotechnology, Forschungszentrum Jülich, 52425 Jülich, Germany*

*Corresponding author:

E-Mail: alexander.gruenberger@uni-bielefeld.de

SI Materials and methods

CFD

Geometry and operating conditions

The geometry was adapted from Probst et al.[1] It has a symmetric design with two supply channels flanking the cultivation chamber. The cultivation chamber was modelled with the exact dimensions shown here, 90 µm width, 80 µm length and 0.8 µm height. It is directly connected to the supply channels that are 100 µm wide, 140 µm long and 10 µm high. Both supply channels are modelled 30 µm upstream and downstream of the cultivation chamber. Inlet and outlet boundary conditions were applied at these positions. Symmetry along a symmetry plane through the cultivation chamber was exploited to reduce computation time. For an additional study, a typical colony of 300 cells were implemented and described as cut out volumes within the chamber. These volumes were inaccessible for the fluid. The boundaries of the cell volumes were equipped with a Monod-sink term.

Simulation setup

Calculations of the stationary velocity field and the transient mass transport were performed using COMSOL Multiphysics 5.4.0.225 (COMSOL AB, Sweden). For the stationary velocity field, the stationary Navier-Stokes equations[2] for an incompressible, isothermal, Newtonian fluid were solved:

$$\mu \nabla^2 \boldsymbol{u} = \nabla p$$

$$\nabla \cdot \boldsymbol{u} = 0$$

where $\boldsymbol{u}$ denotes the fluid velocity vector in m s^{-1}, p the fluid pressure in Pa, and μ the dynamic viscosity in Pa s. The properties of the fluid within the channels and the cultivation chamber were treated as identical to pure water. The parabolic velocity profile at the inlets of the supply channels was applied using the laminar inflow feature of COMSOL Multiphysics with an inflow length of 100 µm. The flow rate at the inlet was set to be 500 nl min^{-1} per supply channel, which means a total flow rate of 6.5 µl min^{-1} for the whole system. For the PDMS and glass walls, the no-slip condition was used.

For the mass transport the diffusion-advection equation according to Deen[2] was applied:

$$\frac{\partial c}{\partial t} + \nabla \cdot (-D \nabla c) + \boldsymbol{u} \cdot \nabla c = 0$$

where c denotes the substrate concentration in mmol L^{-1}, D the binary diffusion coefficient of the solute in water in m^2 s^{-1}, and $\boldsymbol{u}$ the velocity vector in m s^{-1}. The diffusion coefficient of glucose in water is $5.4 \cdot 10^{-10}$ m^2 s^{-1}.[3] A rectangular pulse function with maximum concentration of 222 mmol L^{-1} and a fixed frequency between 0.05 Hz and 5 Hz was imposed as inlet concentration.

A frequency response analysis was conducted by comparing the normalized substrate concentrations measured in the cultivation chamber at a stationary state, with the maximum substrate concertation measured in total denoting 100%. A stationary state was assumed when the amplitudes measured in the cultivation chamber varied less than 1% over five consecutive oscillations. The substrate concentrations in the cultivation chamber were determined using the domain probe feature of COMSOL Multiphysics. The results are presented in a Bode plot.

For the additional study, where the cell colony was implemented, substrate consumption by the organisms was modelled using a flux boundary condition at the cell surfaces. The equation applied for the dependence of the uptake rate on the surrounding glucose concentration is based on Monod assumptions[4]:

$$Q = \hat{Q} \frac{c}{c + K_s}$$

A K_s-value of 4.5 mmol L^{-1} for C. *glutamicum* and glucose according to Wendisch *et al.* was used.[5] The glucose uptake rate per cell dry weight q_G = 4.42 mmol g^{-1} h^{-1} and the single-cell dry weight of $1.5 \cdot 10^{-12}$ g reported by Unthan *et al.* for C. *glutamicum* were used to calculate an uptake rate $\hat{Q}$ of $1.82 \cdot 10^{-7}$ mol m^{-2} s^{-1}.[6]

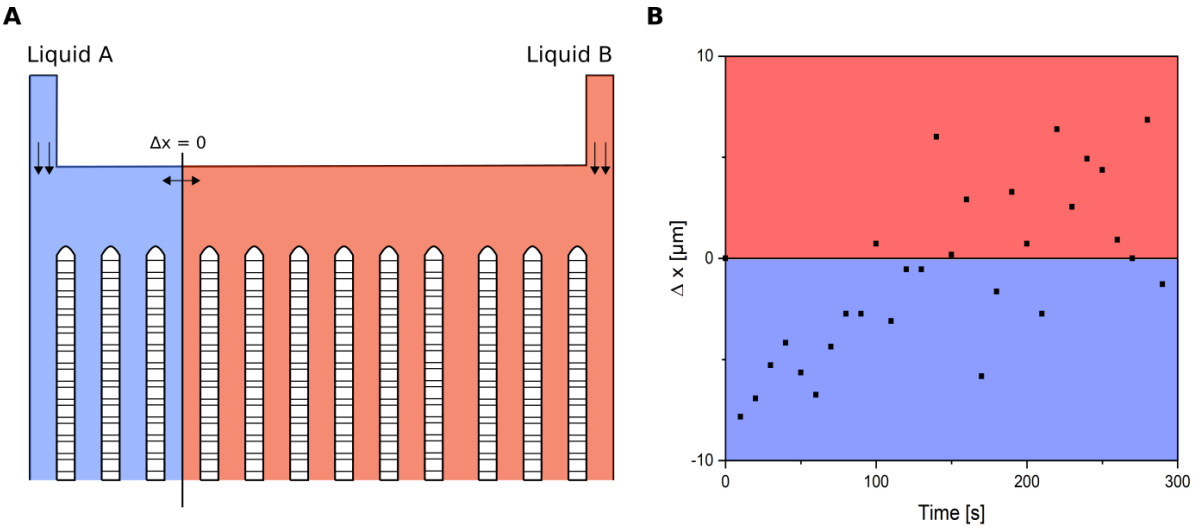

Fig. S1: Displacement of the boundary line between two laminar flows from set point (Δx = 0) at the 10 second oscillation.

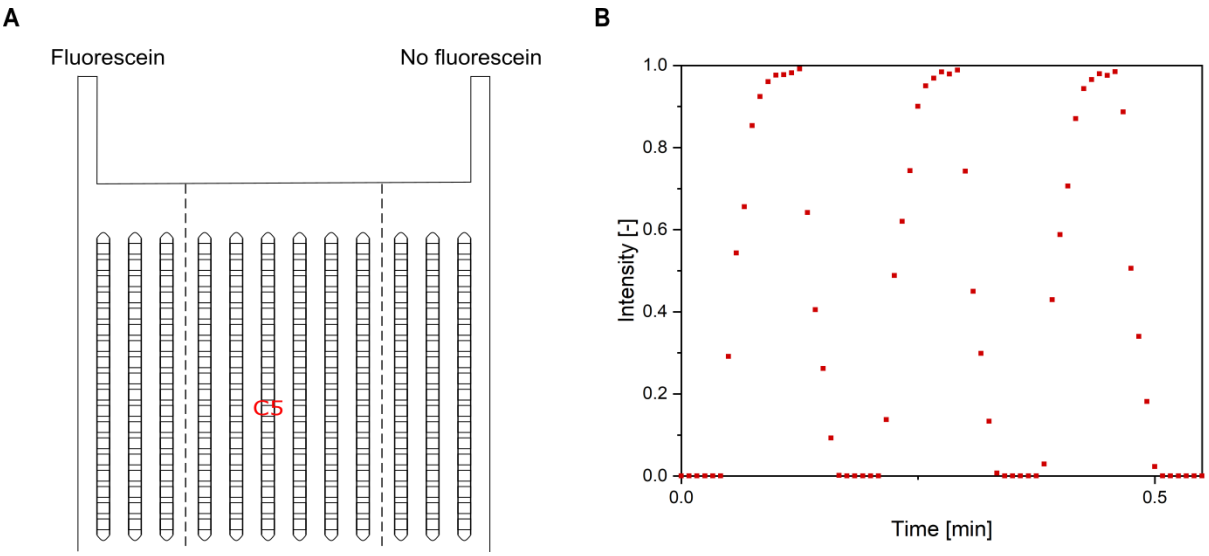

Fig. S2: Result of the experimental validation of the microfluidic device of the 5 second oscillation with fluorescein and ethanol at the position C6.

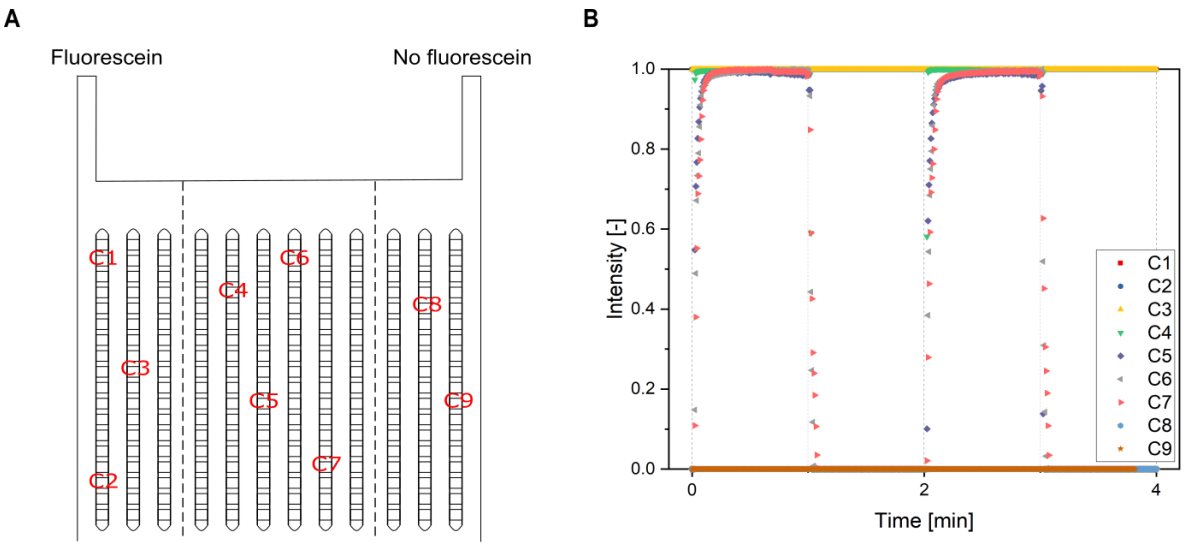

Fig. S3: Experimental validation of the microfluidic device. A) Schematic overview of the microfluidic device with selected cultivation chambers for the analysis of the fluorescence signal. B) Result of the 1 minute oscillation with fluorescein and ethanol for different positions.

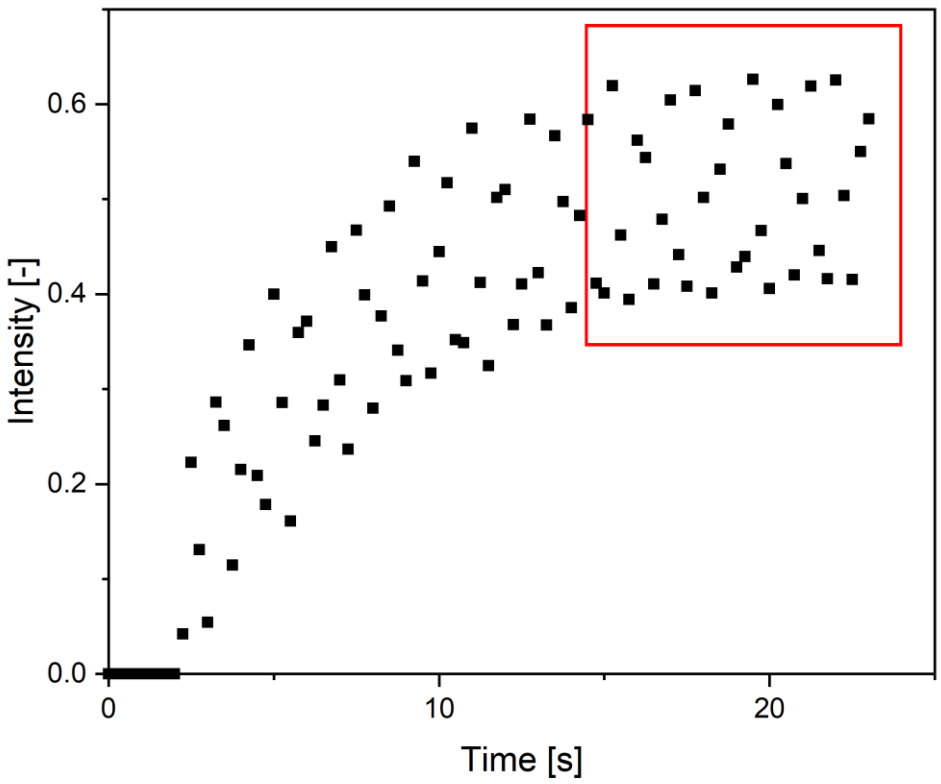

Fig. S4: Transient effect during the 500 ms oscillation. In the red area the average value after the transient oscillation was calculated

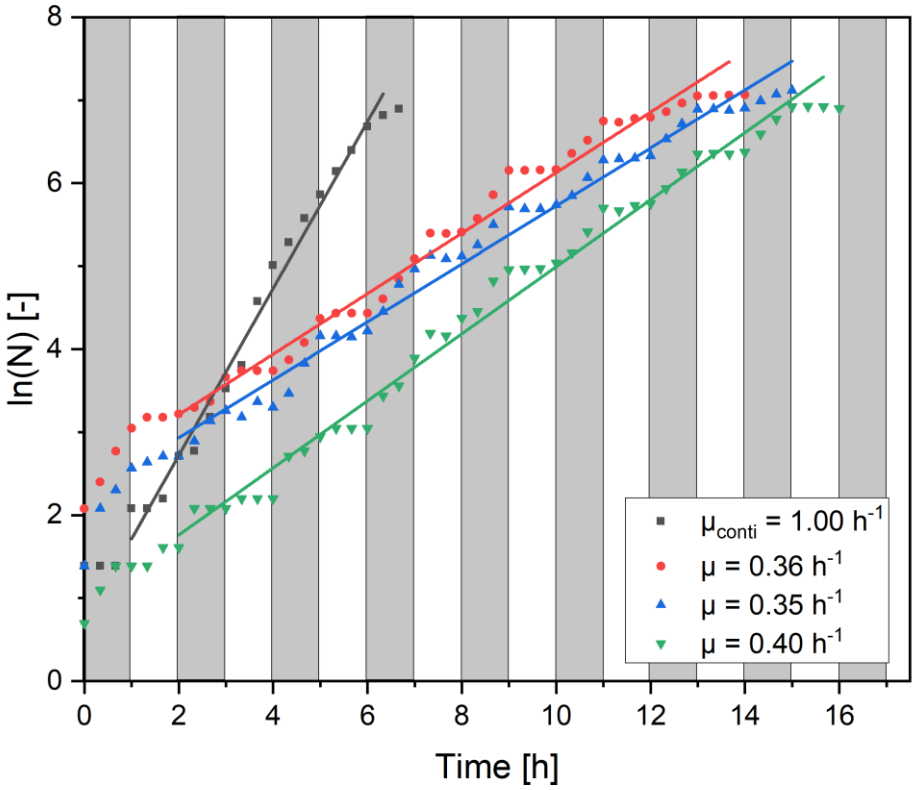

Fig. S5: Growth curves of dMSCC at 60 minute oscillation between BHI medium and PBS buffer with linear regression for the determination of the growth rate (μ_{colony} = (0.37 ± 0.03) h^{-1}). The grey areas show the BHI medium pulses and the white areas the PBS buffer pulses.

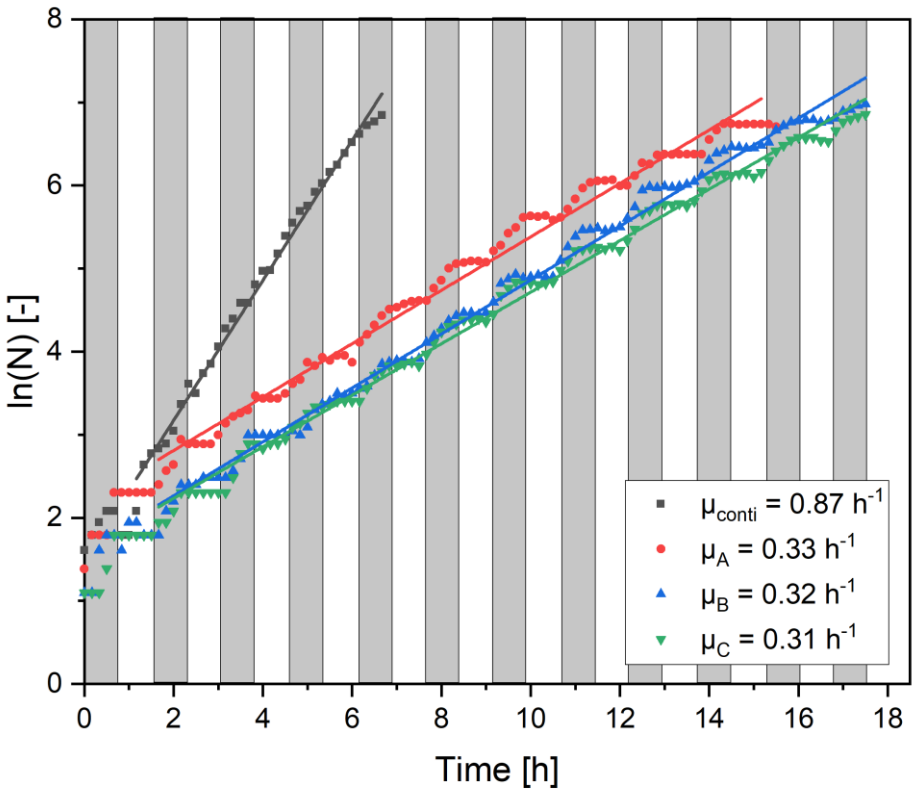

Fig. S6: Growth curves of dMSCC at 45 minute oscillation between BHI medium and PBS buffer with linear regression for the determination of the growth rate (μ_{colony} = (0.32 ± 0.01) h^{-1}). The grey areas show the BHI medium pulses and the white areas the PBS buffer pulses.

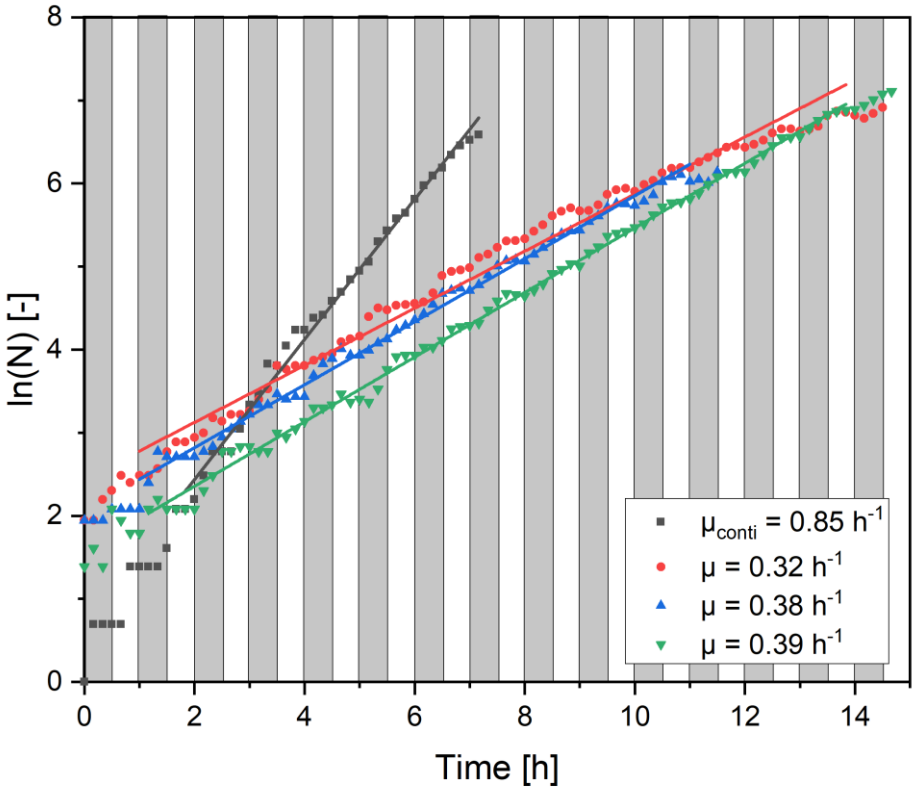

89

90 **Fig. S7**: Growth curves of dMSCC at 30 minute oscillation between BHI medium and PBS
91 buffer with linear regression for the determination of the growth rate (μ_{colony} = (0.36 ± 0.04) h^{-1}).
92 The grey areas show the BHI medium pulses and the white areas the PBS buffer pulses.

93

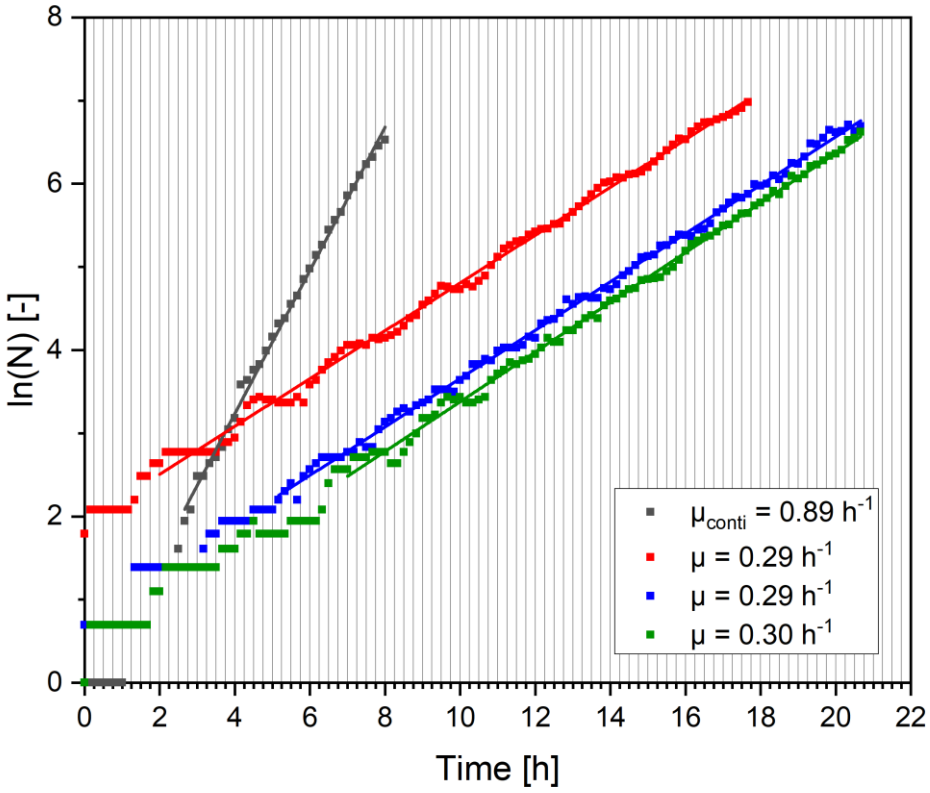

94

95 **Fig. S8**: Growth curves of dMSCC at 15 minute oscillation between BHI medium and PBS
96 buffer with linear regression for the determination of the growth rate (μ_{colony} = (0.29 ± 0.01) h^{-1}).

97

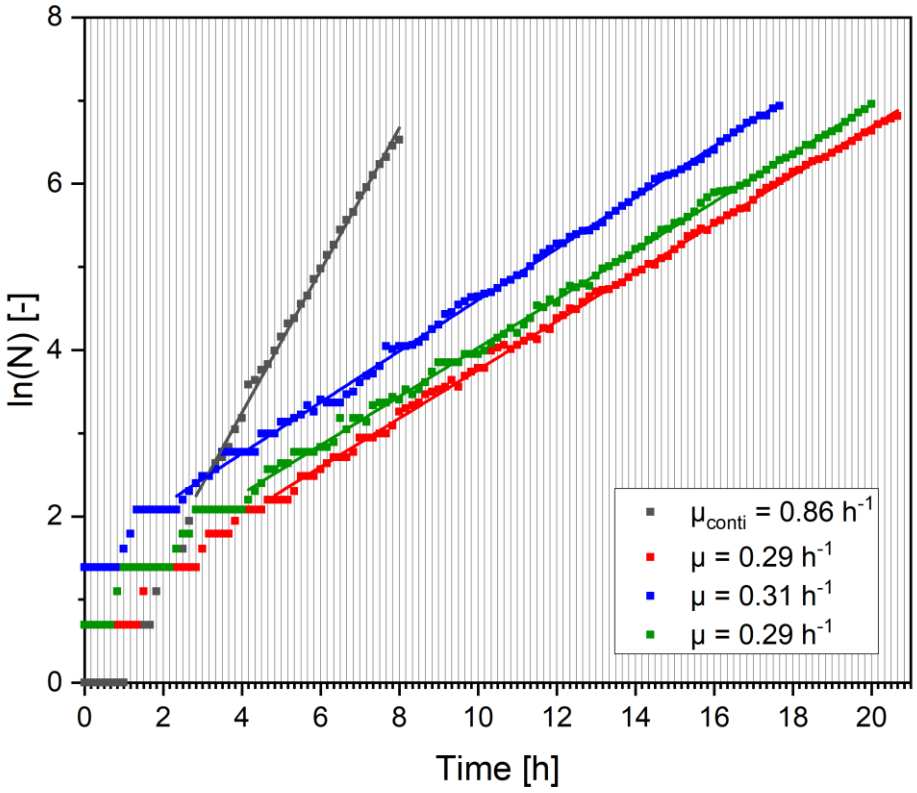

Fig. S9: Growth curves of dMSCC at 10 minute oscillation between BHI medium and PBS buffer with linear regression for the determination of the growth rate (μ_{colony} = (0.30 ± 0.01) h^{-1}).

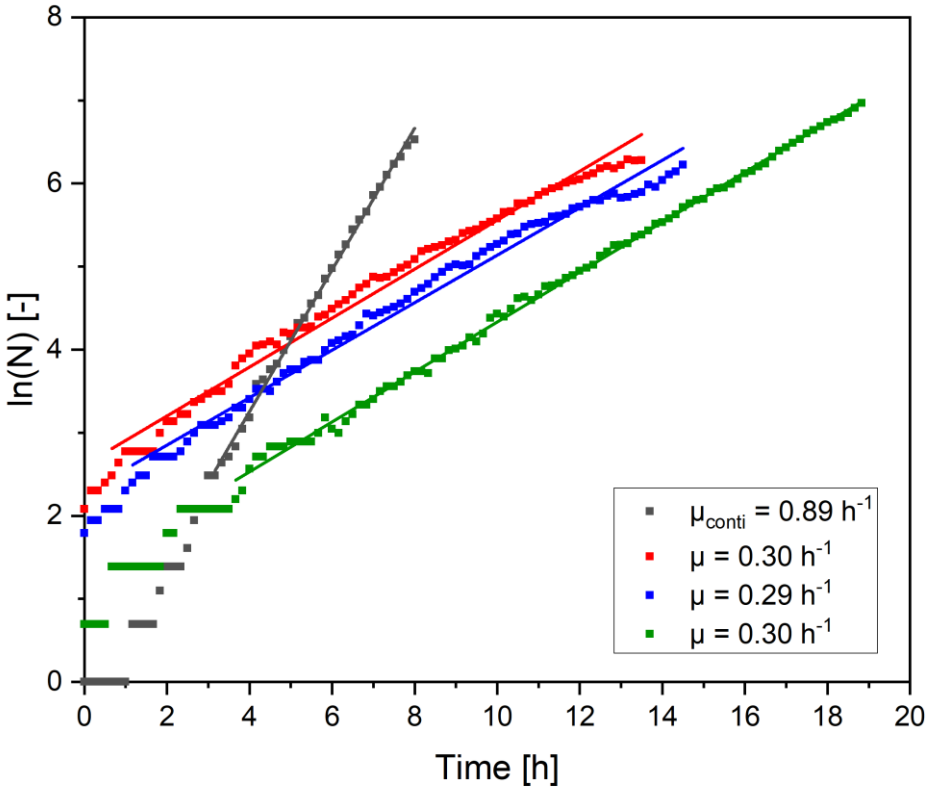

Fig. S10: Growth curves of dMSCC at 5 minute oscillation between BHI medium and PBS buffer with linear regression for the determination of the growth rate (μ_{colony} = (0.30 ± 0.01) h^{-1}).

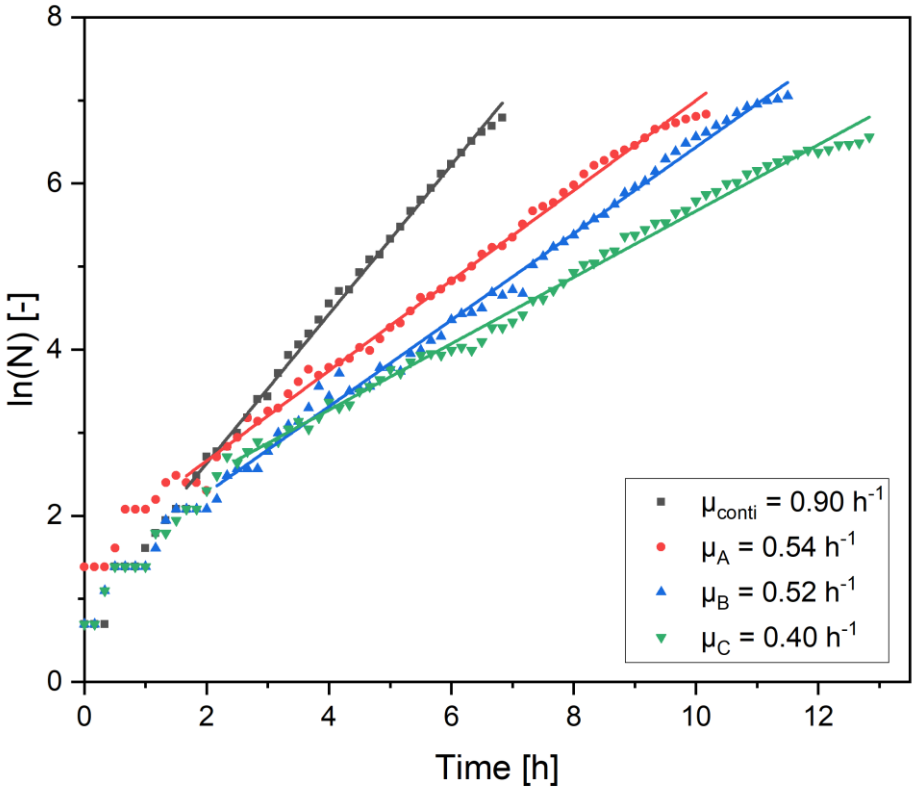

106

107 **Fig. S11**: Growth curves of dMSCC at 1 minute oscillation between BHI medium and PBS
108 buffer with linear regression for the determination of the growth rate (μ_{colony} = (0.49 ± 0.07) h^{-1}).

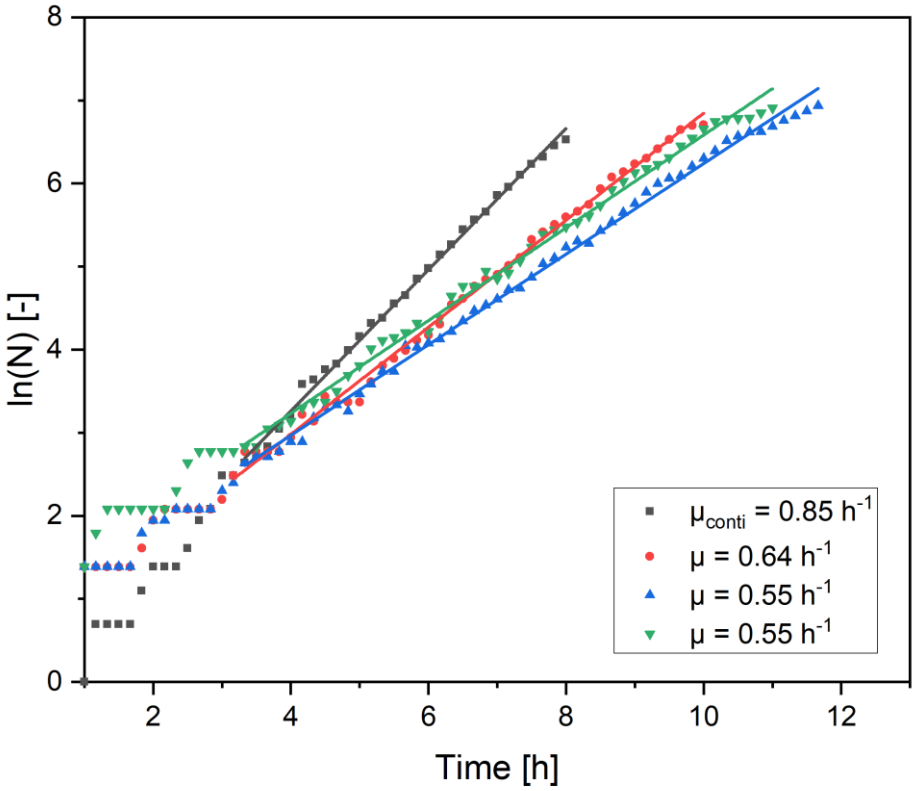

Fig. S12: Growth curves of dMSCC at 20 second oscillation between BHI medium and PBS buffer with linear regression for the determination of the growth rate (μ_{colony} = (0.58 ± 0.05) h^{-1}).

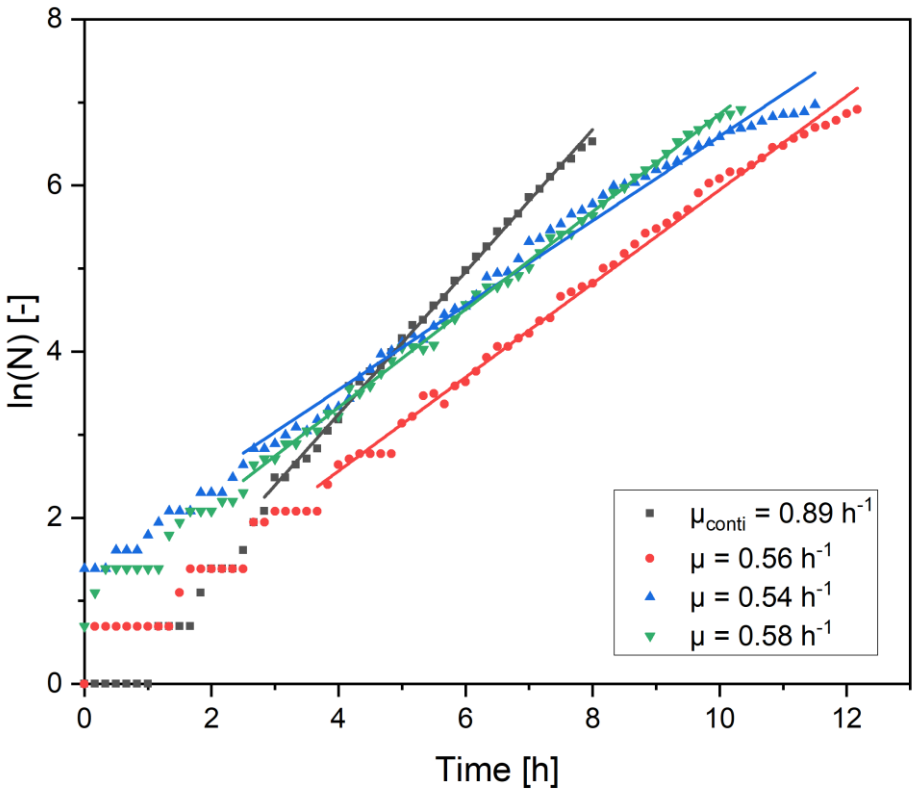

114

115 **Fig. S13**: Growth curves of dMSCC at 10 second oscillation between BHI medium and PBS
116 buffer with linear regression for the determination of the growth rate (μ_{colony} = (0.56 ± 0.02) h^{-1}).

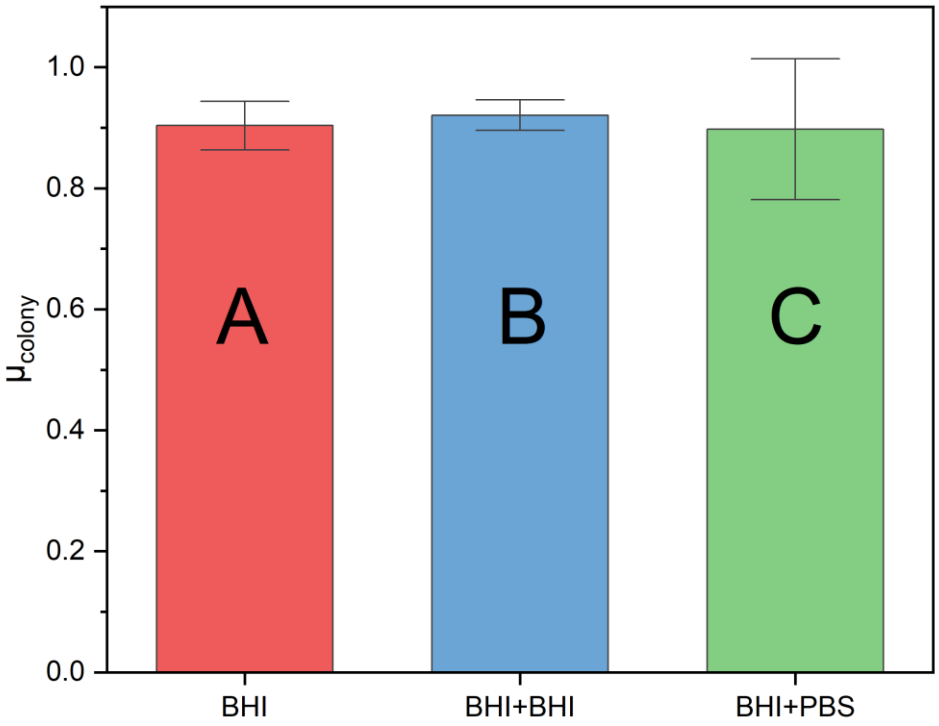

Fig. S14: Overview of different control experiments. A) Continuous cultivation in BHI medium (red). B) 10 second oscillation between BHI medium and BHI medium (blue). C) Continuous cultivation with a 1:1 mixture of BHI medium and PBS buffer (green).

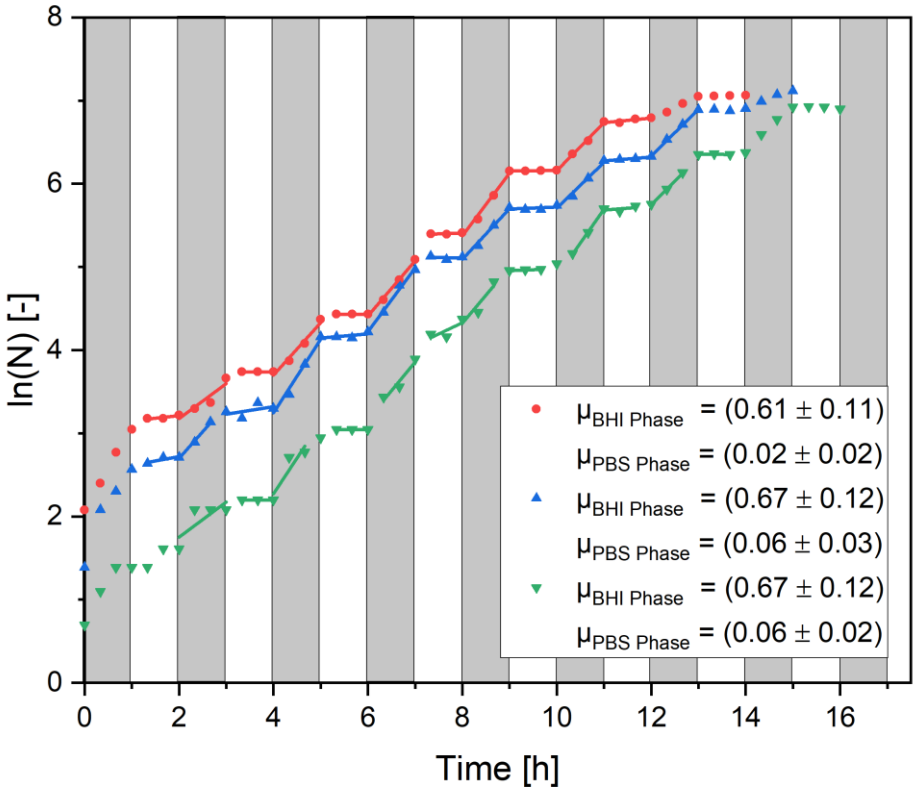

Fig. S15: Growth curves of dMSCC at 1 hour oscillation between BHI medium and PBS buffer with linear regression for the determination of the growth rate during the BHI perfusion phase and PBS perfusion phase.

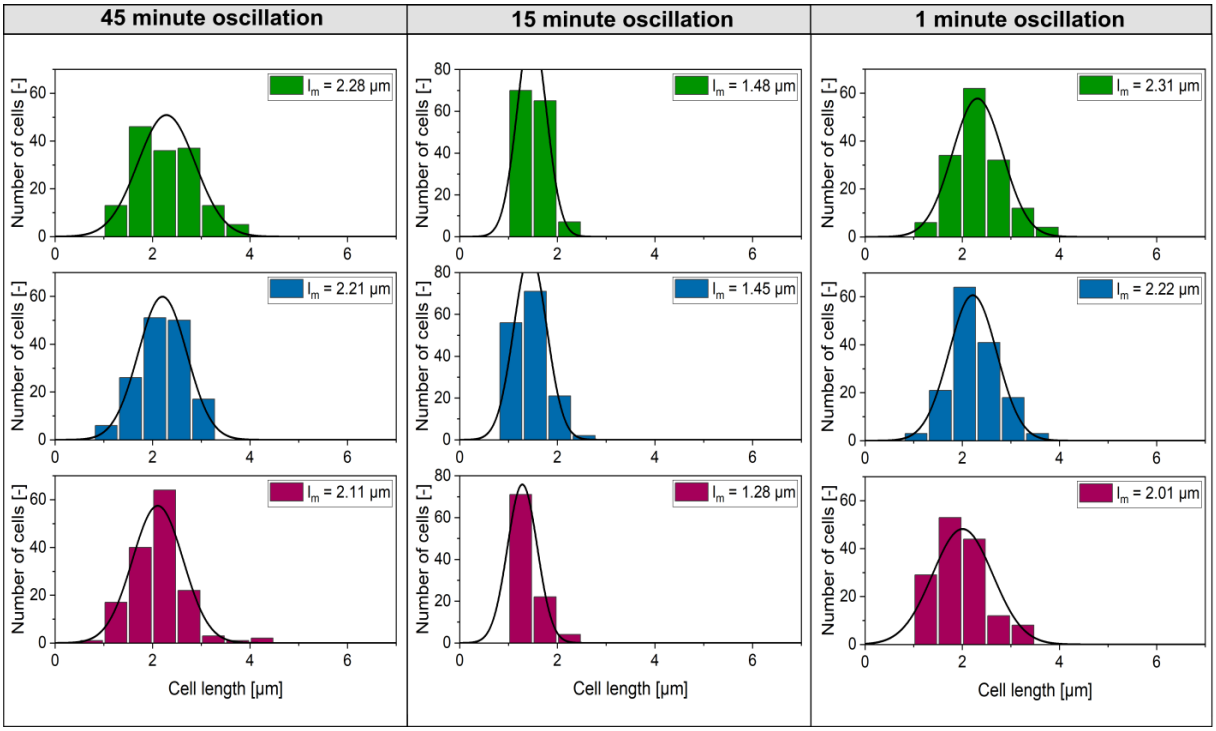

126

127 **Fig. S16**: Cell length histogram of the dMSCC with different oscillations frequencies between
128 BHI medium and PBS buffer after 12 h of cultivation, three colony with N = 150 (green, blue,
129 red).

130

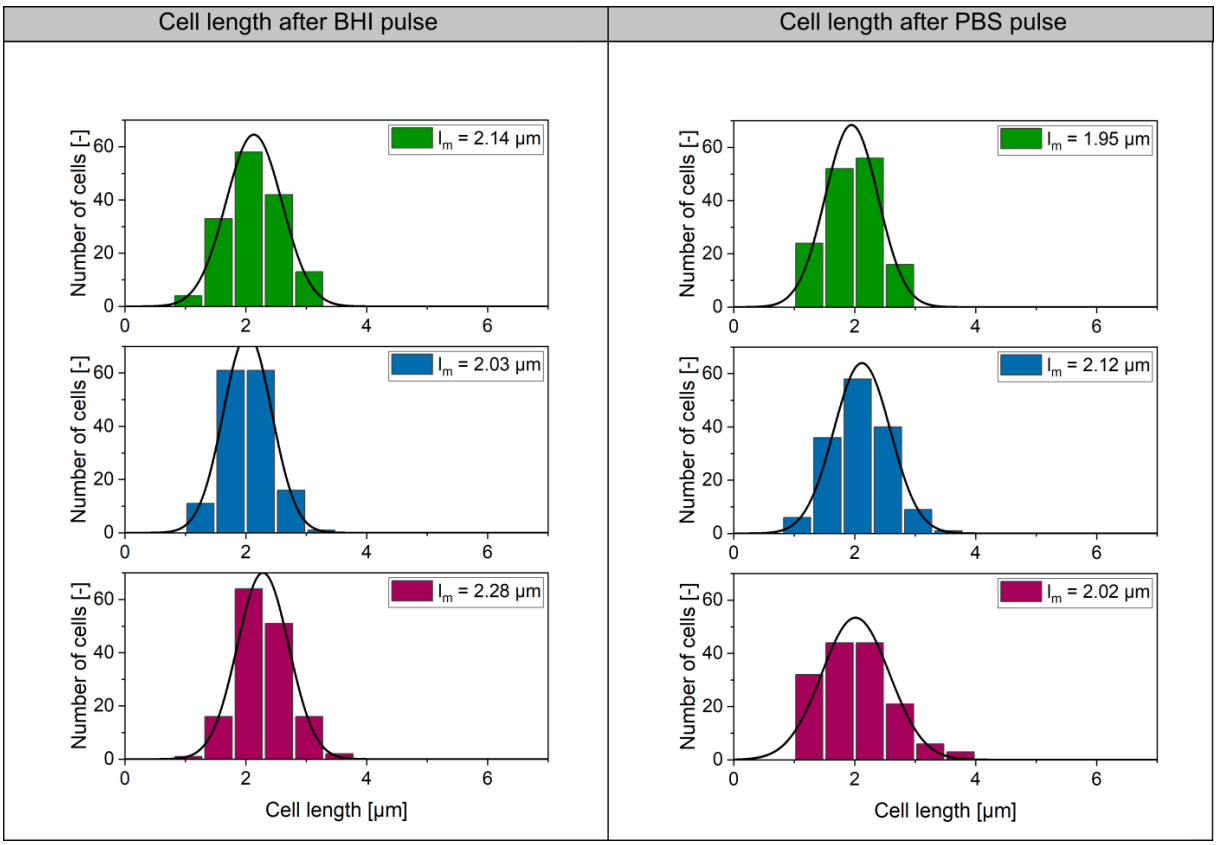

131

Fig. S17: Cell length histogram of the dMSCC for the 30 minute oscillation after BHI pulse and after the PBS pulse after 12 h of cultivation, three colony with N = 150 (green, blue, red).

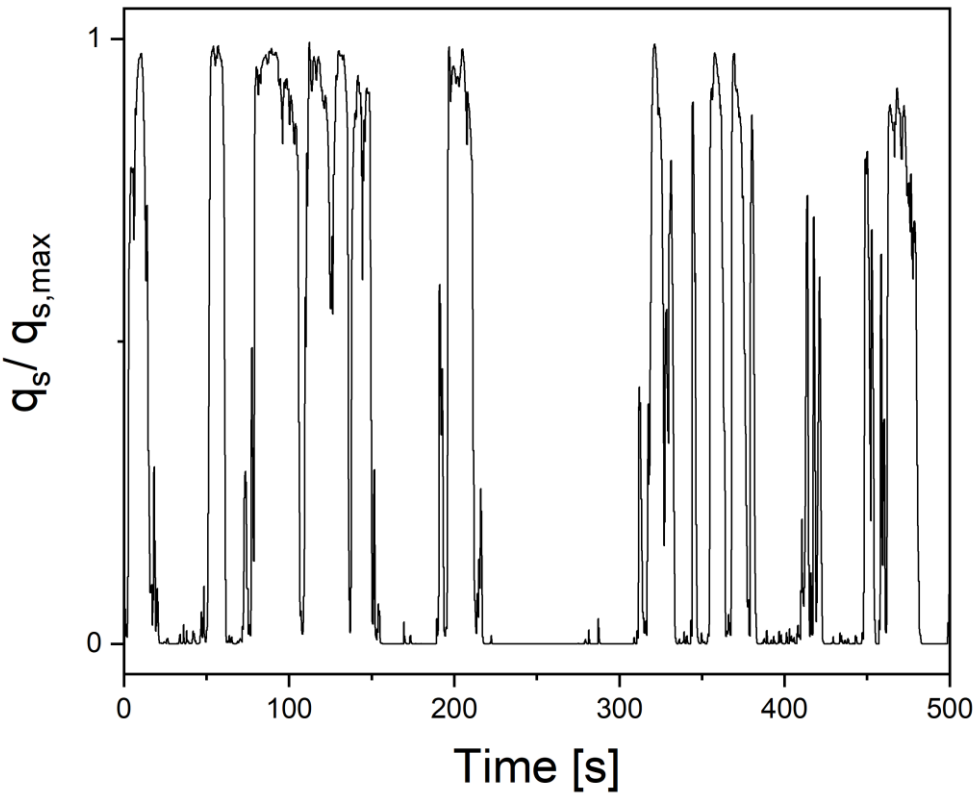

Fig. S18: Typical lifeline of a large-scale bioreactor. Copyright 2020, from Biochemical Engineering Journal. Adapted with permission from Haringa et al.[7]

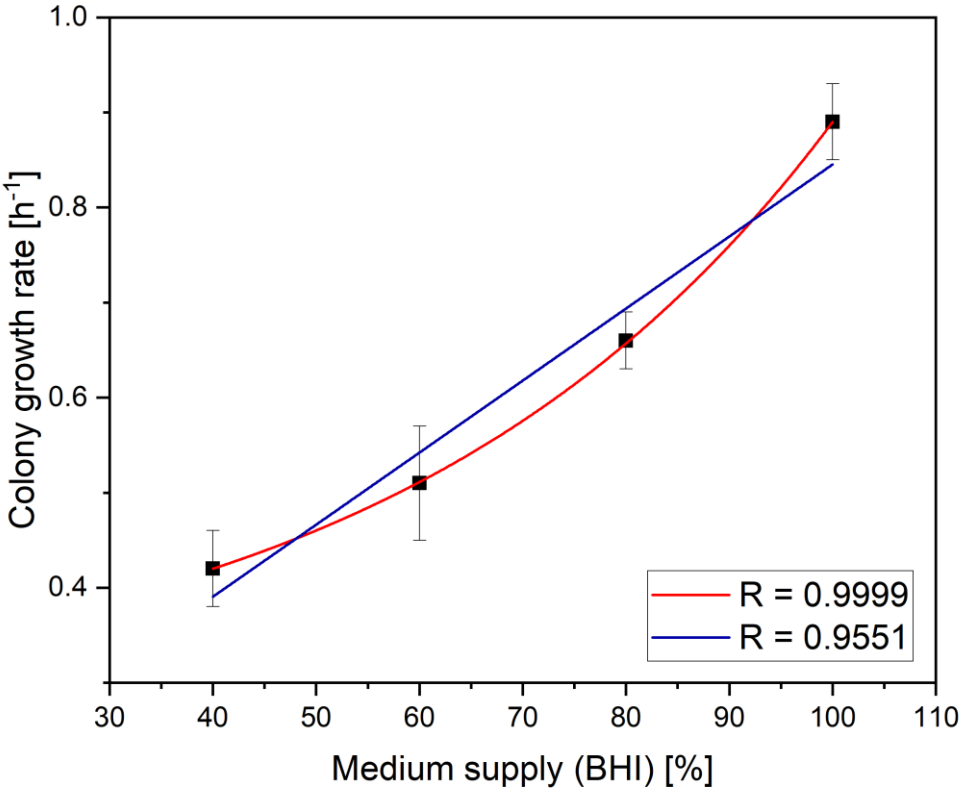

Fig. S19: Correlation analysis between the colony growth rate and the overall medium supply by different experimental lifelines.

References

1 C. Probst, A. Grünberger, N. Braun, S. Helfrich, K. Nöh, W. Wiechert and D. Kohlheyer, *Anal. Methods*, 2015, **7**, 91–98. DOI: 10.1039/C4AY02257B.

2 W.M. Deen, *Analysis of transport phenomena*, Oxford Univ. Press: New York, 1998.

3 C.T. Culbertson, S.C. Jacobson and J.M. Ramsey, *Talanta*, 2002, **56**, 365-373. DOI: 10.1016/s0039-9140(01)00602-6.

4 J. Monod, *Ann Rev Microbiol,* 1949, **3**, 371–394. DOI: 10.1146/annurev.mi.03.100149.002103.

5 V.F. Wendisch, A.A. de Graaf, H. Sahm, B.J. Eikmanns, *J. Bacteriol*., 2000, **182**, 3088–3096. DOI: 10.1128/jb.182.11.3088-3096.2000.

6 S. Unthan, A. Grünberger, J. van Ooyen, J. Gätgens, J. Heinrich, N. Paczia, W. Wiechert, D. Kohlheyer, S. Noack, *Biotech bioeng,* 2014, **111**, 359–371. DOI: 10.1002/bit.25103.

7 C. Haringa, R. F. Mudde and H. J. Noorman, *Biochem Eng J*, 2018, **140**, 57–71. DOI: 10.1016/j.bej.2018.09.001.